



Effects of nano-metakaolin on the enhanced properties and microstructure development of natural hydraulic lime

Zirui Zhu^a, Peng Liu^a, Jinhua Wang^b, Hongbin Zhang^{a,b,*}, Wei Luo^{c,*}

^a Institute for Preservation and Conservation of Chinese Ancient Books, Fudan University Library, Fudan University, Shanghai 200433, China

^b Department of cultural heritage and museology, Fudan University, Shanghai 200433, China

^c State Key Laboratory for Modification of Chemical Fibers and Polymer Materials, College of Materials Science and Engineering, Institute of Functional Materials, Donghua University, Shanghai 201620, China

ARTICLE INFO

Article history:

Received 20 January 2024

Revised 11 March 2024

Accepted 19 March 2024

Available online 20 March 2024

Keywords:

Natural hydraulic lime

Nano-metakaolin

Pozzolanic reaction

Properties

Microstructures

ABSTRACT

Natural hydraulic lime (NHL) has garnered increasing attention for its sustainable and suitable performance in the field of historical building restoration. However, the prolonged hardening time and sluggish hydration rate of NHL influence the workability, strength development, and durability of construction structures in which it is used. In this study, nano-metakaolin (NMK) was applied as a highly reactive supplementary cementitious material (SCM) for NHL-based mortars to enhance their properties with various ratios. Meanwhile, the effects of NMK and its related enhancement mechanism on the physical properties and chemical structures of NHL composites were systematically investigated, mainly involving the modifications in their microstructure, chemical composition, and C-S-H structure. Results demonstrated that NMK-modified samples showed distinct and superior properties to pure NHL sample, such as shorter initial/final setting times (15.1%–49.1%, 27.1%–50.0%), and higher compactness (67.8%–81.4%, 38.1%–44.8%), lower shrinkage (25.0%–56.3%, 12.5%–25.0%), enhanced compressive strength (404.5%–546.0%, 180.8%–354.1%) and flexural strength (227.5%–351.1%, 59.9%–125.7%) for both early and late curing times (7 and 28 days). The inclusion of NMK not only acts as a fine filler, but also promotes NHL's hydrate rate by its super high pozzolanic activity, thus optimizing the pore structures and increasing the content and the average silicate chain length of hydration gel in NHL. Overall, this study can contribute to a deeper understanding of the enhancement mechanism of NMK on the physical properties and chemical structures of NHL from a meso/microscopic perspective, with a view to broadening NHL's potential applications.

© 2025 Published by Elsevier B.V. on behalf of Chinese Chemical Society and Institute of Materia Medica, Chinese Academy of Medical Sciences.

Natural hydraulic lime, as a compatible, eco-friendly inorganic cementitious material, has been widely used in the restoration of culturally and historically significant buildings [1–7]. Typically, NHL is produced by grinding the clayish or siliceous limestone (including chalk) after burning, which can set and harden in both water and air [8,9]. The mineralogical phases of NHL mainly consist of dicalcium silicate (C₂S), which imparts hydraulic property, calcium hydroxide (CH) with air-hardening property, and incompletely burnt calcium carbonate (CaCO₃) [10,11]. Unfortunately, as of now, NHL still suffers from some limitations regarding low hydration activity and high rupture susceptibility, particularly in low-humidity environments [12–14]. These limitations have a significant impact on its workability, strength development, and durability, which restrict its widespread applications.

Extensive research has shown that nano-reinforcing material presents promising applications in hydraulic materials due to its small size, large specific surface area, and strong reactivity, compared to ordinary active minerals, such as fly ash, silica fume, and slag powder [15–17]. Among these nano-sized materials, nano-metakaolin (NMK), a nanoscale laminar silica-aluminate equipped with high pozzolanic activity, has been developed and applied in concrete and cement to enhance their various properties [18,19]. Shoukry *et al.* [20] revealed that NMK accelerates the cement-hardened process, as evidenced by the decrease of CH contents with the increase of NMK replacement amount. M. S. Morsy *et al.* [21] assessed the effect of NMK on the hydration characteristics of fly ash blended cement. The experimental results showed that the compressive and flexural strengths of mortar containing NMK were both higher than those of the pure samples after curing 60 days, which may be attributed to NMK's filling effect and high pozzolanic activity. Collectively, these studies all confirmed the role of NMK in accelerating the hydration reaction for hydraulic ma-

* Corresponding authors.

E-mail addresses: zhanghongbin@fudan.edu.cn (H. Zhang), wluo@dhu.edu.cn (W. Luo).

terials. Correspondingly, the enhancement mechanism of NMK has also been discussed in detail by many researchers. In simple terms, NMK exhibits a rapid chemical reaction rate with CH, effectively raising the filling density of calcium-silicate-hydrate (C-S-H) gels [22,23]. Besides, it can serve as a fine filler to fill and bridge the meso/micropore structures of the sample, reduce its porosity, and then provide a suitable template for C-S-H nucleation and growth to induce hydration, and make it have more dense structure, which is another crucial mechanism for accelerating sample's hydration reaction [24–28].

In general, the hydration process of NHL is similar to that of Portland cement. The development of properties in both NHL and cement is governed by the internal complex evolution of microstructures, which strongly depends on the formation and growth of C-S-H [29,30]. Based on the previous section, it can be inferred that NMK has the potential to improve NHL performance by optimizing the pore structure and facilitating the growth of C-S-H gel chains. Unfortunately, there is a lack of research on nano-metakaolin for natural hydraulic lime, especially in terms of systematic investigation of changes in chemical composition, microstructure, and properties of modified NHL mortars. Such investigations are necessary to advance the current status and future development of NHL's application.

Based on the above speculations, this work investigates the effects of NMK on the properties and microstructure of NHL in order to prepare NHL-based mortar with elevated performances, thereby extending the prospects of NHL in construction applications. Therefore, intensive studies have been conducted to examine the fresh and hardened properties of NHL mortars with different NMK ratios, especially focusing on setting time, fluidity, compactness, shrinkage, and mechanical strength. Furthermore, various microstructural tests, including pore structure analysis, compositional variation, and C-S-H relative content and structural change, are used to raise and discuss the rational mechanism behind the improvement of properties in the modified samples.

The information on raw materials, sample preparation process, and experimental analysis methods are included in the supporting information (Table S1 and Fig. S1 in supporting information). As for raw materials, NHL is mainly composed of the oxides of calcium and silicon and its particle sizes are from 1 μm to 15 μm . The mineralogical phases of NHL are calcium silicate (C_2S), calcium hydroxide (CH), as well as calcite (CaCO_3). NMK exhibits a distinct amorphous nano-lamellar structure with widths ranging from 50 nm to 200 nm. The main oxide components of NMK are Al_2O_3 and SiO_2 .

According to the wt% content of NMK, the prepared samples are denoted as M_0 , M_{10} , M_{20} , and M_{30} , respectively.

Fig. 1 illustrates the various properties of pure NHL and NMK-modified NHL mortars in both fresh and hardened states. As shown in Fig. 1a, the fluidity is decreased a little with the addition of NMK, and their fluidity reduces by ca. 5.2%, 14.6%, and 26.3% respectively, compared with the M_0 fresh mortar. Meanwhile, the initial and final setting times are displayed in Fig. 1b. It is evident that both initial and final setting times are sped up ca. 15.1%/27.1%, 35.8%/40.6%, and 49.1%/50.0% respectively, depending on the pre-added NMK dosage. In view of the nano-size, high chemistry activity, and larger specific surface of NMK, NMK may tend to form more flocculated structures within the mortar, which would reduce the content of free water in the slurry, leading to a decrease in its fluidity [31,32]. Besides, the presence of NMK may accelerate the hydration reaction of NHL due to its pozzolanic activity [33,34], which allows the mortar to complete setting in a shorter time.

Figs. 1c–f show the properties of hardened mortar samples, including compactness, shrinkage, compressive strength, and flexural strength at different curing times. As shown in Fig. 1c, the compactness of NMK-modified mortars, as reflected by the wave velocity, is obviously changed by the addition of NMK. All samples with different NMK contents (10%, 20%, 30%) present higher wave velocity than the pure NHL sample for both early and late curing times (7, 14, 28 days). Interestingly, the NMK-modified mortars exhibit a much faster increase in wave velocity after early curing (7 days). Among them, the most apparent wave velocity increase rate of 81.4% could be observed in M_{20} after only curing 7 days. It means that the addition of NMK can effectively increase the compactness of NHL-based mortars, especially in the early stage.

The shrinkage results of all samples are shown in Fig. 1d. Although the pure NHL sample shows a low shrinkage of only 0.08%, 0.13%, and 0.24% after curing for 7, 14, and 28 days respectively, the addition of NMK can further reduce the shrinkage of NHL-based mortars for both early and late curing times (7, 14, 28 days). The most effective sample is M_{20} , with the smallest shrinkage of only 0.04%, 0.08%, and 0.18% for curing 7, 14, and 28 days respectively. The possible reason may be attributed to the “filler effect” and strong pozzolanic activity of NMK, which can refine the pore structure of NHL-based samples to hinder their shrinkage. However, the excess of NMK may produce partial agglomeration, which reduces the filling of smaller-sized pores and does not prevent sample shrinkage adequately, as in the case of M_{30} .

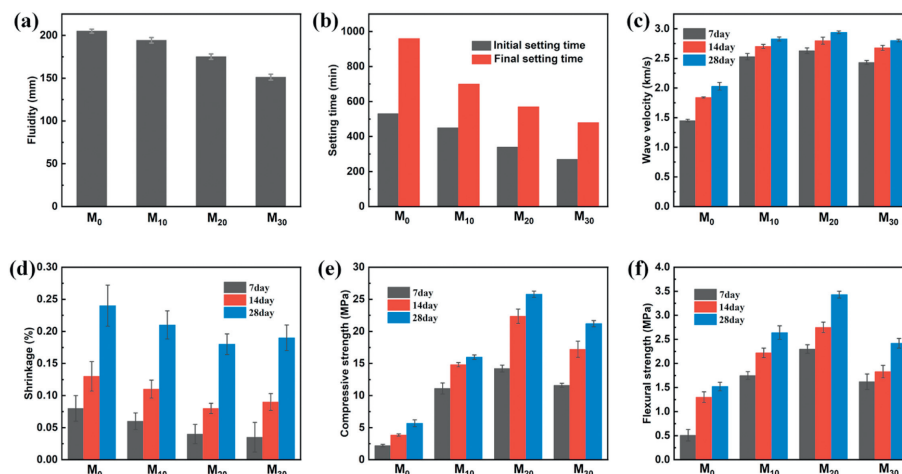


Fig. 1. The properties of NHL-based mortars. The fresh mortars: (a) Fluidity, (b) setting time. The hardened mortars: (c) Compactness, (d) shrinkage, (e) compressive strength, and (f) flexural strength.

The mechanical strength is essential to the NHL-based samples in a hardened state, which highly affects its applicability and durability for construction. As depicted in Figs. 1e and f, the compressive and flexural strengths of the pure NHL mortar are initially very low, reaching only 2.20/3.86/5.68 MPa and 0.51/1.30/1.52 MPa respectively, for curing the age of 7/14/28 days. The addition of NMK can largely strengthen the mechanical properties of hardened NHL-based mortars. Both the compressive and flexural strengths increase with the dosages of NMK (10%, 20%), but show a slight decrease when the content reaches 30%. The most effective sample is M_{20} , and it displays the maximum compressive and flexural strengths of 14.21/22.35/25.79 MPa and 2.30/2.75/3.43 MPa for curing 7/14/28 days respectively. Compared to M_0 , the 7-days early compressive and flexural strengths of M_{20} increase by ca. 546.0% and 351.1%, and the 28-days strengths increase by ca. 354.1% and 125.7% respectively. Apparently, the incorporation of NMK has greatly enhanced the mechanical strength of NHL at an early stage, both in compressive and flexural strength, which may provide guarantees for its practical engineering construction and later performance maintenance. As a well-established fact, the mechanical property of NHL, as a porous hydraulic mortar, is primarily influenced by the hydrated gel content and pore structure. By acting as a fine and superhigh pozzolanic supplementary cementitious material (SCM), NMK may fill the smaller gaps inside NHL and produce more contents of C-S-H gel by pozzolanic reaction, which will optimize their pore structures.

Research has confirmed that the characteristics of inorganic cementitious materials, including natural hydraulic lime, are predominantly dependent on the transformation of phase and pore structure during hardening [35,36]. Consequently, investigating alterations in the pore structure of NMK-modified NHL samples and the creation and advancement of its hydration products, such as C-S-H gels and CH crystals, can help reveal the improvement mechanism of nano-metakaolin particles on properties of NHL.

In view of the low structural activity of C_2S and the very slow reaction of CH and CO_2 in the air [37,38], a schematic (Fig. 2) is tried to summarize for illustrating the microscopic changes in NMK-modified NHL mortar during the hydration process. This process can be divided into three parts: (1) Dissolution of NHL raw materials, where soluble ions such as Ca^{2+} and OH^- enter the solution and alter its composition. (2) First hydration reaction, where C-S-H continues to grow on the surface of C_2S and NMK. Except for the hydration of C_2S , here high-activity NMK reacting with CH from the NHL will result in the generation of C-S-H or C-S(A)-H, and play an important role in the early strength. (3) Second hydration reaction, where the newly generated CH from C_2S hydration

and NHL dissolution undergoes further pozzolanic reaction with excess NMK, additionally increasing the hydration production content. Throughout the hydration process described above, the chemical interaction between NMK and NHL leads to changes in mortar composition, meanwhile the growth of C-S-H gel would alter the pore structure within the sample. Moreover, the structure of C-S-H may also be influenced by NMK. The combination of these changes impacts the hardening properties of NHL mortar. These microscopic changes and their implications are discussed in detail below.

Fig. 3 demonstrates the pore size distribution of samples at different curing stages. The MIP results (Figs. 3a-c) illustrate that the pore sizes of all samples are primarily distributed within two ranges. The range of 10–200 nm corresponds to the capillary pores inside the mortar, while the range of 1000–5000 nm is related to the air voids [39]. Among them, the pore size distribution of NHL without NMK is mainly around 3000 nm. In contrast, samples introduced with NMK exhibit a higher optimized pore structure compared to pure NHL. This is supported by an increase in the pore volume below 100 nm and a gradual decrease in the pore volume in the range of 1000–5000 nm. Of particular interest, as the NMK content reaches 20%, not only does the content of capillary pores inside sample increase, but it also moves towards smaller pore sizes around 20 nm. The increased smaller pore content and pore size refinement of NHL are mainly attributed to the nanoscale size and pozzolanic activity of NMK, resulting in more hydration products filling the pores. Additionally, the MIP analysis presents a notable increase in the content of pore volume below 10 nm, which is associated with C-S-H gel pores in NHL-based samples [40]. However, due to the limitations of the MIP test range, nitrogen physical adsorption tests will be performed in the following section to assess the micro/mesopore characteristics of the NMK-modified samples.

Exploring the distribution of micro/mesopore pores, especially those smaller than 10 nm, is instructive in assessing the hydrate degree of NMK-modified mortars as it is commonly acknowledged that in hydraulic mortar, C-S-H gel particles are interconnected during hydration to form gel pores with sizes less than 10 nm [41]. The results of the nitrogen adsorption and desorption test provide valuable insights. Fig. S2 (Supporting information) demonstrates that all samples exhibit a combination of type II and IV adsorption curves, accompanied by a visible capillary condensation phenomenon. This indicates that the samples mainly consist of mesopore (2–50 nm) and macropore (>50 nm) structures, with a relatively smaller amount of micropores (<2 nm). Pore size distributions of NHL mortar with or without NMK at different ages are

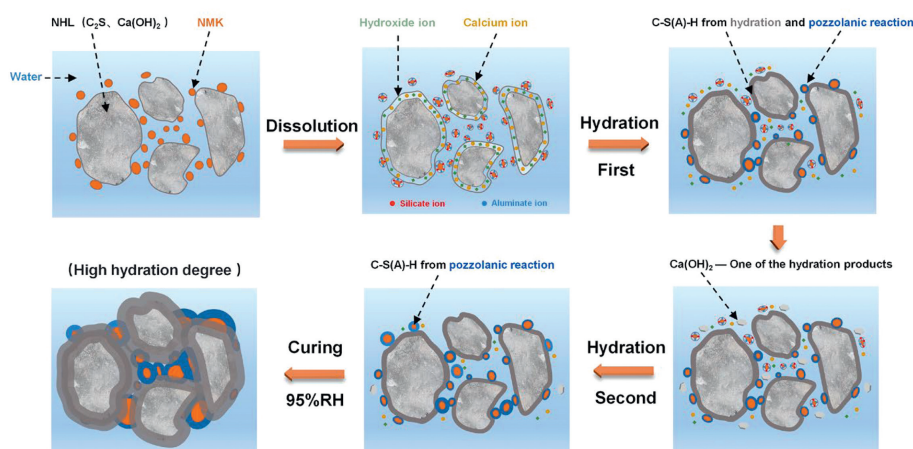


Fig. 2. Schematic diagram of the hydration process of NMK-modified NHL mortar.

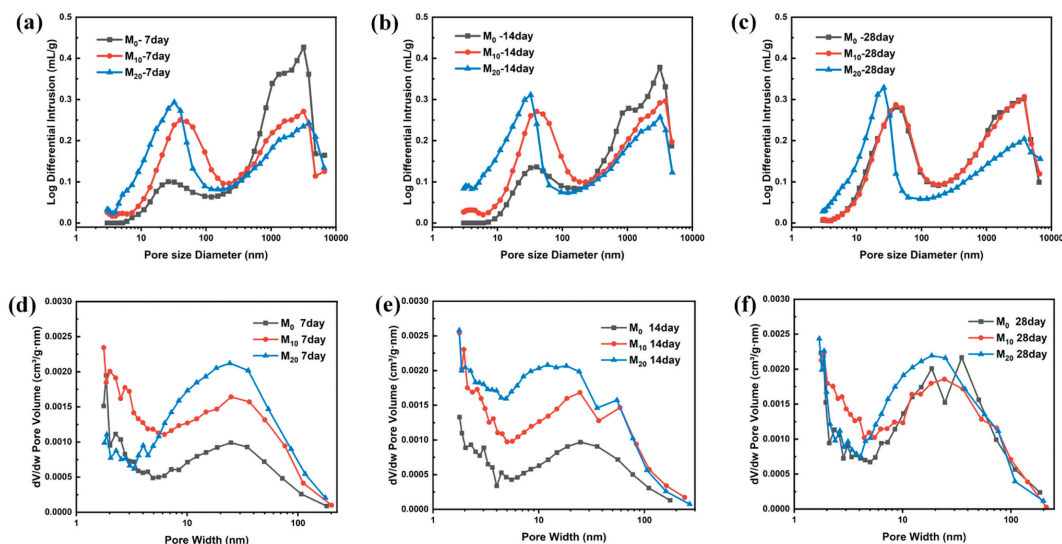


Fig. 3. Pore size distribution of samples with different curing times: MIP (a) 7 days, (b) 14 days, (c) 28 days. Nitrogen adsorption: (d) 7 days, (e) 14 days, (f) 28 days.

shown in Figs. 3d–f. It is distinctly observed that the incorporation of NMK significantly increases the content of pores smaller than 10 nm within the samples. This indicates that NMK effectively promotes the hydration rate of NHL, resulting in an increase in the hydration product C–S–H gel, particularly in the early stages. By expanding the volume of hydrated gel, there is a corresponding increase in the mechanical strength of the modified samples.

Scanning electron microscopy (SEM) was used to observe the microscopic morphology of modified samples at different curing ages, and the distribution of hydration products and micron-sized pore structures on the samples can be distinctly seen in Figs. 4a–f. Some holes and a small amount of mesh and needle-like products on the surface of the NMK-free sample can be seen in Fig. 4a. The mesh and needle-like products can be identified as C–S–H by the EDS analysis in Fig. S3a (Supporting information). Some CaCO_3 chunks can also be detected. As the NMK content increases, the number and size of holes decrease, while the mesh-like products gradually increase for M_{10} and M_{20} , where it is difficult to observe the presence of holes (Fig. 4c). After curing 14 days, there are a small number of holes still present in M_0 , indicating the low degree of hydration. On the other hand, M_{10} and M_{20} display a denser structure with increased mesh gels, which is mainly attributed to the high pozzolanic activity of the NMK. Meanwhile, as shown in Figs. S3b and c (Supporting information), some calcium aluminate silicate hydrate (C–S(A)–H) gels may be observed on the surface of modified samples as a result of the reactive aluminum in NMK, which alters the structure of C–S–H.

The XRD patterns of hardened samples at the age of 7, 14, and 28 days are shown in Figs. 4g–i. The phase of samples is mainly composed of CH, CaCO_3 , and monocarboalunminate ($\text{C}_4\text{ACH}_{11}$). While C–S–H gel is not indexed by XRD due to its poor crystalline properties [42]. The XRD results illustrate that the relative intensity of CH characteristic peaks in M_0 shows an increase and then a decreased trend with curing. This is due to the fact that NHL produces hydration products CH during hardening, increasing its content. These CH then decrease when undergo carbonation in air at later stages. Besides, M_0 would generate a small amount of $\text{C}_4\text{ACH}_{11}$ at the age of 28 days, a hydration product containing aluminum [43,44]. The addition of NMK accelerates the decrease of the relative intensity of CH characteristic peaks. In composite samples, NMK can react with CH to produce a more hydrated calcium silicate gel, which promotes the development of their internal microstructure. In particular, the presence of $\text{C}_4\text{ACH}_{11}$ characteristic

peak can be clearly observed both in the M_{10} and M_{20} , even at the age of 7 days, which is due to the reaction between the alumina in NMK and NHL [45]. That also illustrates the enhancement of NMK on the hydration reaction of NHL.

Fourier transform infrared spectroscopy (FT-IR) was used to test and further verify the improvement of NMK on NHL hydration reactions, and the results are shown in Figs. 4j–l. All samples of different ages exhibit the same absorption peaks at 3660, 1430, 980, 875, and 710 cm^{-1} . Among these peaks, the one at around 3660 cm^{-1} corresponds to the stretching vibration of hydroxyl in CH [3]. The absorption bond at approximately 980 cm^{-1} is associated with the Si–O stretching vibration of C–S–H [46,47]. The peaks near 1430, 875, and 710 cm^{-1} represent characteristic peaks of CaCO_3 , which correspond to the stretching vibration of C–O, the bending vibration of CO_3^{2-} , and the bending vibration of O–C–O, respectively [48,49]. The FT-IR results revealed that, at the early stage, NMK effectively reduces the peak intensity of CH in the NHL through pozzolanic reaction, resulting in the production of more hydrate products. Similarly, the increased intensity of the C–S–H characteristic peak in the mortars containing NMK also proves that NMK may have the effect of promoting NHL hydrate reaction.

C–S–H, the primary product of NHL after hydration, consists of calcium planes and silica chains on both sides, together with water molecules, hydroxyl groups, and some calcium ions (Fig. 5a). The structure of C–S–H gels is significantly affected by the alteration of the silica chains that occurs during hydration, which can be detected by ^{29}Si NMR [50]. Typically, the different peaks in ^{29}Si NMR patterns (Fig. 5b) can be denoted as Q^n ($n = 0, 1, 2, 3, 4$) in relation to the chemical environment of silicon ions, where Q^0 , Q^1 and Q^2 refer to silicon monomers, dimers and middle chain groups, respectively [51]. In addition, the presence of aluminum may also influence the chemical shift of ^{29}Si [52], such as Q^2 (1Al), potentially altering the structure of C–S–H.

Fig. 5c shows the ^{29}Si NMR spectra of the unhydrated NHL. There are three peaks at around $-70\sim-75$ ppm, which are related to the various crystalline structures of C_2S . For NMK, three main peaks at -85.2 ppm for Q^4 (3A1), -95.5 ppm for Q^4 (2A1), and -108.5 ppm for Q^4 (1A1) can be detected in Fig. 5d. The ^{29}Si NMR spectra of the pure NHL sample at the age of 14 days is shown in Fig. 5e, where several new peaks appear, belonging to Q^1 and Q^2 (1A1) and Q^2 , respectively. In particular, the peak intensity of Q^1 is apparently higher than that of Q^2 , indicating that the C–S–H gel formed at the early stage is dominated by dimers. The doping of

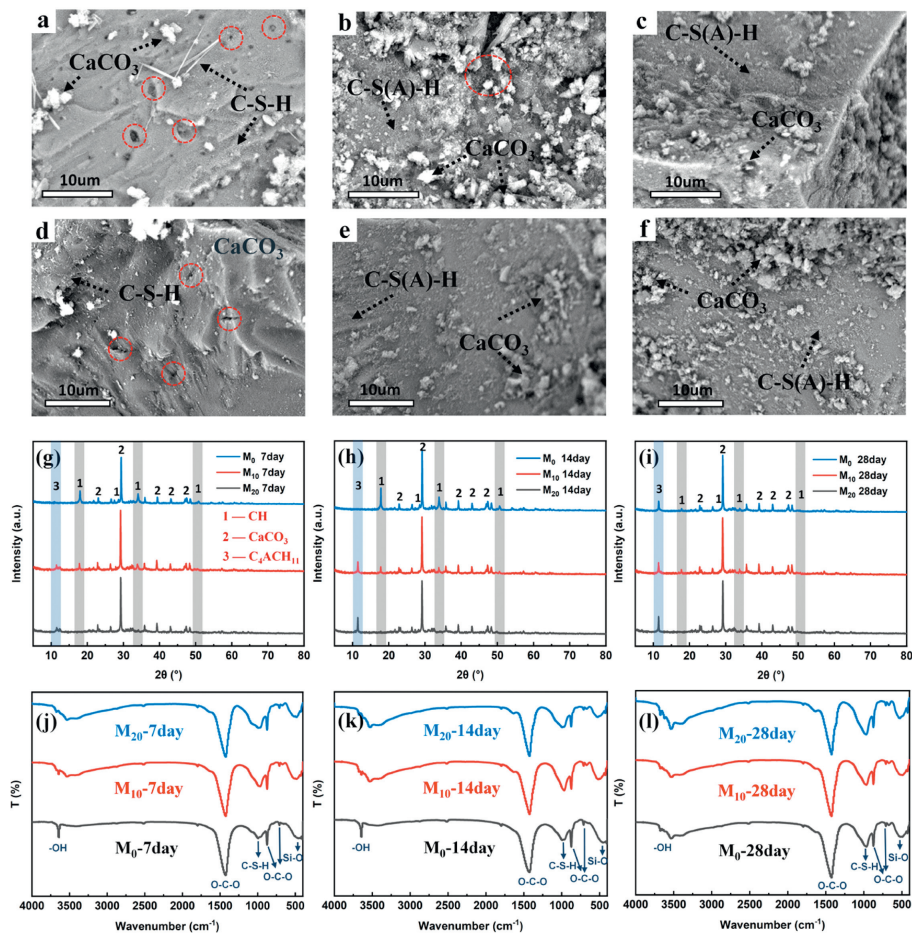


Fig. 4. The SEM of different samples: (a) M₀, (b) M₁₀, (c) M₂₀ for curing 7 days; (d) M₀, (e) M₁₀, (f) M₂₀ for curing 14 days. The XRD patterns of samples with different curing times: (g) 7 days, (h) 14 days, (i) 28 days. The FT-IR patterns of samples with different curing times: (j) 7 days, (k) 14 days, (l) 28 days.

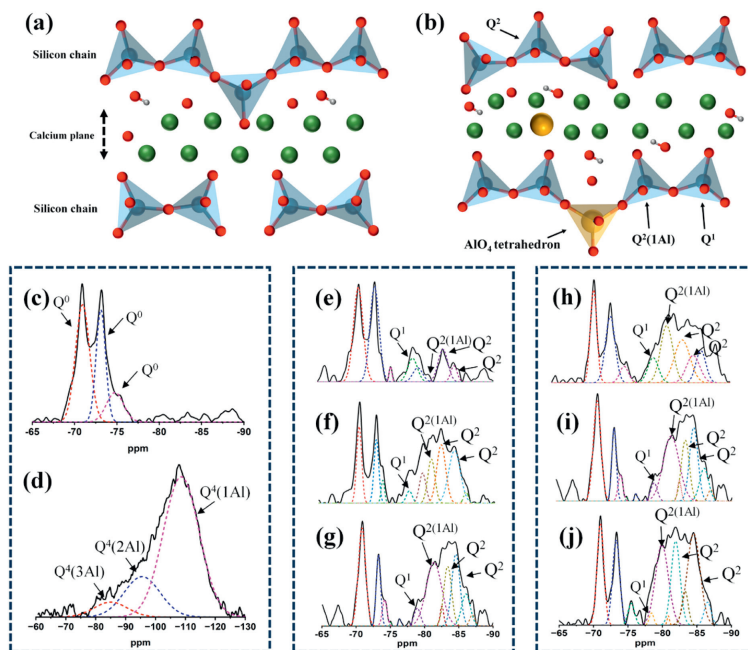


Fig. 5. (a, b) The structure of C-S-H and C(A)-S-H. Spheres of blue, yellow, green, red, and gray colors represent Si, Al, Ca, O, and H, respectively. The results and fitting peaks of ²⁹Si NMR: Raw materials (c) NHL-5, (d) NMK; (e) M₀, (f) M₁₀, and (g) M₂₀ at age of 14 days; M₂₀ at age of (h) 7 days, (i) 14 days, and (j) 28 days.

NMK, on the other hand, greatly enhances the peak intensity of Q^2 (1A1) and Q^2 , both of M_{10} and M_{20} (Figs. 5f and g). This illustrates that NMK can effectively accelerate the hydration reaction of NHL and enhance the polymerization degree of C–S–H gels, according to its “filler effect” and pozzolanic activity. Meanwhile, the increase in the peak intensity of Q^2 (1A1) displays that more AlO_4 tetrahedrons are doped into the silicon chains, which further promotes the length of chains in the C–S–H. Figs. 5h–j depict the variations in ^{29}Si NMR spectra of M_{20} as a function of curing time (7, 14, and 28 days). The results reveal that the M_{20} exhibits higher relative peak intensities of Q^2 (1A1) and Q^2 , even at the age of 7 days, compared to pure NHL after curing 14 days. This implies that NMK has the effect of promoting early hydration of NHL. Besides, with the curing time increased, the relative peak intensity of Q^2 (1A1) and Q^2 in M_{20} are continued to rise. The decrease in Q^1 peak intensity, accompanied by the increase in Q^2 (1A1) and Q^2 , suggests that the C–S–H gel in M_{20} exhibits characteristics of long-chain structure. Moreover, the entanglement between the long chains contributes to the strength development in the early stage of the sample.

In conclusion, we report on the effects of NMK on the enhanced performance and microstructure development of NHL. The introduction of NMK considerably enhanced the performance of NHL mortars. Compared to pure NHL, the composite mortars with NMK exhibit reduced setting time, higher compactness, lower shrinkage, and enhanced mechanical strength. Early improvements in performance are particularly evident in modified NHL mortars, especially in compressive and flexural strength at an early stage (7 days), which increases by approximately 546.0% and 351.1% respectively, at best. During the hardening process, NMK was inserted into the pores within NHL and then produced additional C–S–H by multiple chemical reactions to further fill internal pores, contributing to the pore size refinement and strength development. Besides, NMK promotes the hydration rate of C_2S while increasing the average silicate chain length of C–S–H. The presence of Al likewise increases the polymerization degree of the hydrated products, which largely contributes to the improvements in the sample's macroscopic properties.

Declaration of competing interest

The authors declare that there is no conflict of interests regarding the publication of this paper.

Acknowledgments

This work was sponsored by National Key R&D Program of China (No. 2021YFC1523403), Guangxi Key Technologies R&D Program (No. AB22080102), Shanxi Provincial Cultural Relics Protection Science and Technology Program (No. 208141400241), and Special Key Project of Chongqing Technology Innovation and Application Development (No. CSTB2022TIAD-KPX0095).

Supplementary materials

Supplementary material associated with this article can be found, in the online version, at doi:10.1016/j.ccl.2024.109794.

References

- [1] M. Apostolopoulou, P.G. Asteris, D.J. Armaghani, et al., *Cem. Concr. Res.* 136 (2020) 106167.
- [2] J. Lanas, J.L. Pérez Bernal, M.A. Bello, et al., *Cem. Concr. Res.* 34 (2004) 2191–2201.
- [3] J. Zhu, J. Hui, H. Luo, et al., *Cem. Concr. Compos.* 122 (2021) 104052.
- [4] M. Destefani, L. Falchi, E. Zendri, *Coatings* 13 (2023) 1418.
- [5] D. Frankeová, V. Koudelková, *Constr. Build. Mater.* 264 (2020) 120205.
- [6] P. Maravelaki-Kalaitzaki, A. Bakolas, I. Karatasios, et al., *Cem. Concr. Res.* 35 (2005) 1577–1586.
- [7] C. De Nardi, A. Cecchi, L. Ferrara, et al., *Compos. Part B: Eng.* 124 (2017) 144–157.
- [8] D. Zhang, J. Zhao, D. Wang, et al., *Constr. Build. Mater.* 186 (2018) 42–52.
- [9] J. Grilo, A.S. Silva, P. Faria, et al., *Constr. Build. Mater.* 51 (2014) 287–294.
- [10] P. Kozlovcev, J. Válek, *Mater. Struct.* 54 (2021) 217.
- [11] J. Válek, E. van Halem, A. Viani, et al., *Constr. Build. Mater.* 66 (2014) 771–780.
- [12] E. Durgun, H. Manzano, R.J.M. Pellenq, et al., *Chem. Mater.* 24 (2012) 1262–1267.
- [13] J. Grilo, P. Faria, R. Veiga, et al., *Constr. Build. Mater.* 54 (2014) 378–384.
- [14] J.S. Pozo-Antonio, *Constr. Build. Mater.* 77 (2015) 472–478.
- [15] K. Luo, J. Li, Z. Lu, et al., *Constr. Build. Mater.* 216 (2019) 119–127.
- [16] P. Maravelaki-Kalaitzaki, Z. Agioutantis, E. Lionakis, et al., *Cem. Concr. Compos.* 36 (2013) 33–41.
- [17] A. Douba, S. Ma, S. Kawashima, *Cem. Concr. Compos.* 125 (2022) 104301.
- [18] P.M. Zhan, Z.H. He, Z.M. Ma, et al., *J. Build. Eng.* 30 (2020) 101259.
- [19] K. Al-Jabri, H. Shoukry, *Constr. Build. Mater.* 177 (2018) 210–221.
- [20] H. Shoukry, M.F. Kotkata, S.A. Abo-El-Enain, et al., *Constr. Build. Mater.* 112 (2016) 276–283.
- [21] Q. Li, Y. Fan, S.P. Shah, *J. Build. Eng.* 77 (2023) 107484.
- [22] S.A. Abo-El-Enain, M.S. Amin, F.I. El-Hosiny, et al., *HBR J* 10 (2014) 64–72.
- [23] S.M.A. El-Gamal, F.S. Hashem, M.S. Amin, *Constr. Build. Mater.* 146 (2017) 531–546.
- [24] J. Xie, H. Zhang, L. Duan, et al., *Constr. Build. Mater.* 256 (2020) 119393.
- [25] Q. Li, Y. Fan, *Constr. Build. Mater.* 353 (2022) 129062.
- [26] M.S. Morsy, H. Shoukry, M.M. Mokhtar, et al., *Constr. Build. Mater.* 172 (2018) 243–250.
- [27] Y. Asghari, S.E. Mohammadyan-Yasouj, S.S. Rahimian Koloor, *Constr. Build. Mater.* 389 (2023) 131605.
- [28] A.S. Fariad, S.A. Mostafa, B.A. Tayeh, et al., *J. Build. Eng.* 43 (2021) 102569.
- [29] Z. Zhang, G.W. Scherer, A. Bauer, *Cem. Concr. Res.* 107 (2018) 85–100.
- [30] D. Zhang, J. Zhao, D. Wang, et al., *Constr. Build. Mater.* 244 (2020) 118360.
- [31] N.A. Tregger, M.E. Pakula, S.P. Shah, *Cem. Concr. Res.* 40 (2010) 384–391.
- [32] D. Zhang, D. Xu, H. Liu, et al., *J. Build. Eng.* 62 (2022) 105351.
- [33] Y. Rechtes, *Constr. Build. Mater.* 175 (2018) 483–495.
- [34] M.S. Muhd Norhasri, M.S. Hamidah, A. Mohd Fadzil, et al., *Constr. Build. Mater.* 127 (2016) 167–175.
- [35] C. Lian, Y. Zhuge, S. Beecham, *Constr. Build. Mater.* 25 (2011) 4294–4298.
- [36] D. Shanmugavel, R. Dubey, R. Ramadoss, *J. Build. Eng.* 30 (2020) 101252.
- [37] S.N. Ghosh, P.B. Rao, A.K. Paul, et al., *J. Mater. Sci.* 14 (1979) 1554–1566.
- [38] V. Nežerka, Z. Slížková, P. Tesárek, et al., *Cem. Concr. Res.* 64 (2014) 17–29.
- [39] D.A. Silva, V.M. John, J.L.D. Ribeiro, et al., *Cem. Concr. Res.* 31 (2001) 1177–1184.
- [40] J. Sun, W. Zhang, J. Zhang, et al., *Constr. Build. Mater.* 280 (2021) 122477.
- [41] J. Yang, G. Zhao, H. Yin, et al., *Appl. Surf. Sci.* 639 (2023) 158159.
- [42] L. Black, K. Garbev, P. Stemmermann, et al., *Cem. Concr. Res.* 33 (2003) 899–911.
- [43] D.P. Bentz, P.E. Stutzman, F. Zunino, *Mater. Struct.* 50 (2017) 173.
- [44] B. Lothenbach, K. Scrivener, R.D. Hooton, *Cem. Concr. Res.* 41 (2011) 1244–1256.
- [45] F. Zunino, K. Scrivener, *Cem. Concr. Res.* 140 (2021) 106307.
- [46] M.U. Okoronkwo, F.P. Glasser, *Mater. Struct.* 49 (2016) 3569–3577.
- [47] A. Nonat, J.C. Mutin, X. Lecoq, et al., *Solid State Ion.* 101–103 (1997) 923–930.
- [48] O. Mikhailova, A. del Campo, P. Rovnanik, et al., *Cem. Concr. Compos.* 99 (2019) 32–39.
- [49] J. Feng, S. Qian, *Mater. Des.* 225 (2023) 111549.
- [50] S. Masse, H. Zanni, J. Lecourtier, et al., *Cem. Concr. Res.* 23 (1993) 1169–1177.
- [51] G.Le Saoût, M. Ben Haha, F. Winnefeld, et al., *J. Am. Ceram. Soc.* 94 (2011) 4541–4547.
- [52] Y. Yan, B. Ma, G.D. Miron, et al., *Cem. Concr. Res.* 162 (2022) 106957.